Int. J. Electrochem. Sci., 5 (**2010**) 668 - 681

International Journal of ELECTROCHEMICAL SCIENCE
www.electrochemsci.org

Preparation of Palladium Particles-decorated Manganese Dioxide and Its Catalysis towards Oxygen Reduction Reaction (ORR)

Keqiang Ding

College of Chemistry and Materials Science, Hebei Normal University, Shijiazhuang 050016, China
*E-mail: dkeqiang@263.net

Received: 29 March 2010 / *Accepted:* 15 May 2010 / *Published:* 30 May 2010

Firstly, manganese dioxides were electrodeposited on a graphite electrode by cyclic voltammetry (CV) from an aqueous solution of 0.1 M Na_2SO_4 containing 5 mM $MnSO_4$, and then the palladium (Pd) particles were prepared onto the resultant MnO_2 by a potentiostatic method. Scanning electron microscopy (SEM) and energy dispersive X-ray analysis (EDX) were used to characterize the resultant samples, and it is demonstrated that Pd coated MnO_2 composites (denoted as Pd/MnO_2) are successfully fabricated for the first time. Lastly, the Pd/MnO_2 modified graphite electrode is employed toward oxygen reduction reaction (ORR), revealing that the catalysis of Pd/MnO_2 composites for ORR is superior to that of the pure MnO_2 material. Also, the possible catalysis mechanism of Pd/MnO_2 for ORR is proposed based on our data. Presenting a novel material of Pd/MnO_2 and verifying its electrocatalysis for ORR are the main contributions of this preliminary work.

Keywords: Cyclic voltammetry (CV); Manganese oxides; Palladium particles; Oxygen reduction reaction (ORR).

1. INTRODUCTION

Recently platinum (Pt) nanoparticles [1-3] have been widely investigated due to its key applications in fuel cell. However, the high loading of Pt in electrodes is a critical obstacle limiting the wide commercialization of fuel cells [4, 5] since Pt is scarce and expensive. Thus, non-platinum based catalysts used in fuel cells were greatly explored with an intention to find an ideal candidate for Pt. Among these candidates reported so far, palladium particles, especially in alkaline media, were recognized as the ideal non-platinum catalysts for oxygen reduction reaction (ORR) [6], methanol oxidation reaction (MOR) [7], and ethanol oxidation reaction (EOR) [8]. For example, Zhang [9] synthesized carbon-supported Pd–Co alloy electrocatalysts, and found that the optimal heat-treatment temperature in the synthesis of Pd-Co alloys was 300 ℃. Wong [10] reported the preparation of palladium nanoplates array (PdNPA) directly grown on a gold substrate, and addressed that PdNPA electrode showed extraordinary electrocatalytic activity towards MOR.

To immobilize Pd particles on a surface, also to meet the commercialization demand, many substrates were utilized to anchor Pd particles. For instance, Takasu [11] prepared Pd particles onto a glassy carbon electrode, and then probed its catalysis for the oxidation of formaldehyde. Abrantes [12] studied the electrochemical nucleation and growth process of palladium particles on polyaniline by chronoamperometry, topographic and phase-mode atomic force microscopy (AFM). Stimming [13] investigated the electrochemical reactivity of nano-islands of palladium on Au (111) towards hydrogen reduction, in which some negative results were obtained. Howbeit, to the best of our knowledge, so far there is no paper reporting the immobilization of Pd particles onto MnO_2.

Oxygen reduction reaction (ORR) is the employed cathode reaction in all kinds of fuel cells including proton exchange membrane fuel cell (PEMFC), direct methanol fuel cell (DMFC) and direct ethanol fuel cell (DEFC), therefore, developing catalysts for ORR has become into an interesting research field recently. In 1973, the phenomenon that manganese oxides can catalysis ORR has been reported by Zoltowski [14]. Recently, Mao [15] et al. pointed out that γ–MnOOH exhibited the best catalysis for ORR among the employed manganese oxides, i.e., Mn_2O_3, Mn_3O_4 and Mn_5O_8, by investigating the catalysis of different kinds of manganese oxides towards ORR. Also, we did some works on the electrochemical preparation and applications of MnO_2 [16-19], and strongly supported that MnO_2 has catalysis towards ORR. However, the exact catalysis mechanism of manganese oxides towards ORR still remains suspended owing to the lack of direct proofs. Thus, improving the catalysis performance of manganese oxides towards ORR are the main tasks for electrochemistry researchers, e.g., very recently, Prof. Ohsaka [20] electrodeposited gold nanoparticles onto a manganese oxide-modified glassy carbon electrode, generating an Au/MnO_2-modified glassy carbon electrode, from a 0.5 M Na_2SO_4 solution containing 1.0 mM $Na[AuCl_4]$ by liner sweep voltammetry (LSV) method rather than a potentiostatic method. To our knowledge, so far, no paper about the palladium particles modified manganese oxides, i.e., Pd/MnO_2, was published.

In this work, cyclic voltammetry (CV) was employed in the preparation of manganese oxides, and then palladium particles were electrodeposited onto the surface of the resultant MnO_2 by a potentiostatic method, forming a Pd/MnO_2 film. SEM images and EDX spectra demonstrated that a Pd-modified MnO_2 was successfully prepared by our proposed method. Lastly, the obtained Pd/MnO_2-coated graphite electrode was employed for ORR, indicating that the electrocatalysis performance of Pd/MnO_2-coated graphite electrode was superior to that of the MnO_2-modified graphite electrode, implying that it is possible to use this Pd/MnO_2 composite material to modify the electrode used in fuel cells. The possible mechanisms were investigated by using electrochemical impedance spectroscopy (EIS), and the catalysis of Pd/MnO_2 composite towards ORR was also proposed.

2. EXPERIMENTAL PART

2.1 Chemicals

The graphite electrode employed was procured from Tianjin Aida Co., Ltd (China). Manganese sulfate, sodium sulfate and other reagents were obtained from Tianjin Chemical Reagent Co. Ltd (China). All chemicals were used as received without further purification and all aqueous solutions were prepared using redistilled water.

2.2 Characterization

Scanning electron microscopy (SEM) was performed on a Hitachi (S-570) micro-scope (Japan) operated at 20kV. Electron dispersive X-ray analysis (EDX, PV-9900, USA) was analyzed by a WD-8X software established by Wuhan University (China). Cyclic voltammetry (CV) and electrochemical impedance spectroscopy (EIS) were conducted on a CHI 660B electrochemical workstation (Shanghai Chenhua Apparatus, China). EIS measurement was performed in the frequency range from 1 to 10^5 Hz with an amplitude of 5 mV.

2.3 Preparation of Pd/ MnO_2-modified graphite electrode

The preparation of manganese oxides was carried out on a CHI 660B electrochemical workstation (Shanghai Chenhua Apparatus, China) connected to a personal computer. A three-electrode configuration was used, in which a graphite electrode (diameter is 6 mm) was used as the working electrode, a platinum foil (area is 1 cm^2) as the counter electrode and saturated calomel electrode (SCE) as the reference electrode.

The graphite electrode was polished with ultrafine SiC paper, degreased with acetone and cleaned with distilled water successively. And then the graphite electrode was electrochemically cleaned in a solution of 0.5 M H_2SO_4, i.e., potential scanning was applied to the graphite electrode in the potential range from -0.2V to 1.2 V versus SCE at a scan rate of 100 mV s^{-1}, during which a wire of platinum and a saturated calomel electrode (SCE) were utilized as the counter and reference electrode, respectively. Prior to the further measurement, the well-treated electrode was washed again by redistilled water in an ultrasonic bath, and dried at room temperature.

Manganese oxides were electrodeposited onto a graphite electrode at room temperature from an aqueous solution of 0.1 M Na_2SO_4 containing 5 mM $MnSO_4$ by CV, the potential sweep rate was 20 mVs^{-1}, the potential range was from 0.4 V to 1.5 V versus SCE. After electrodeposition, the MnO_2-modified graphite electrode (denoted as MnO_2-modified graphite electrode) was thoroughly rinsed by redistilled water and dried in air.

Electrodeposition of palladium particles onto the MnO_2-modified graphite electrode was performed by a potentiostatic method, i.e., the electrode potential of MnO_2-modified graphite was kept to at -0.3 V vs SCE for 300 s in a 0.1 M Na_2SO_4 solution containing 5 mM $MnSO_4$ and 5 mM $PdCl_2$.

Prior to ORR experiment, the electrolyte of 0.1 M Na_2SO_4 was purged by nitrogen gas for 20 min, and then it was bubbled with oxygen gas for at least 20 min to form a oxygen-saturated 0.1 M Na_2SO_4 solution, as described in our previous work [21].

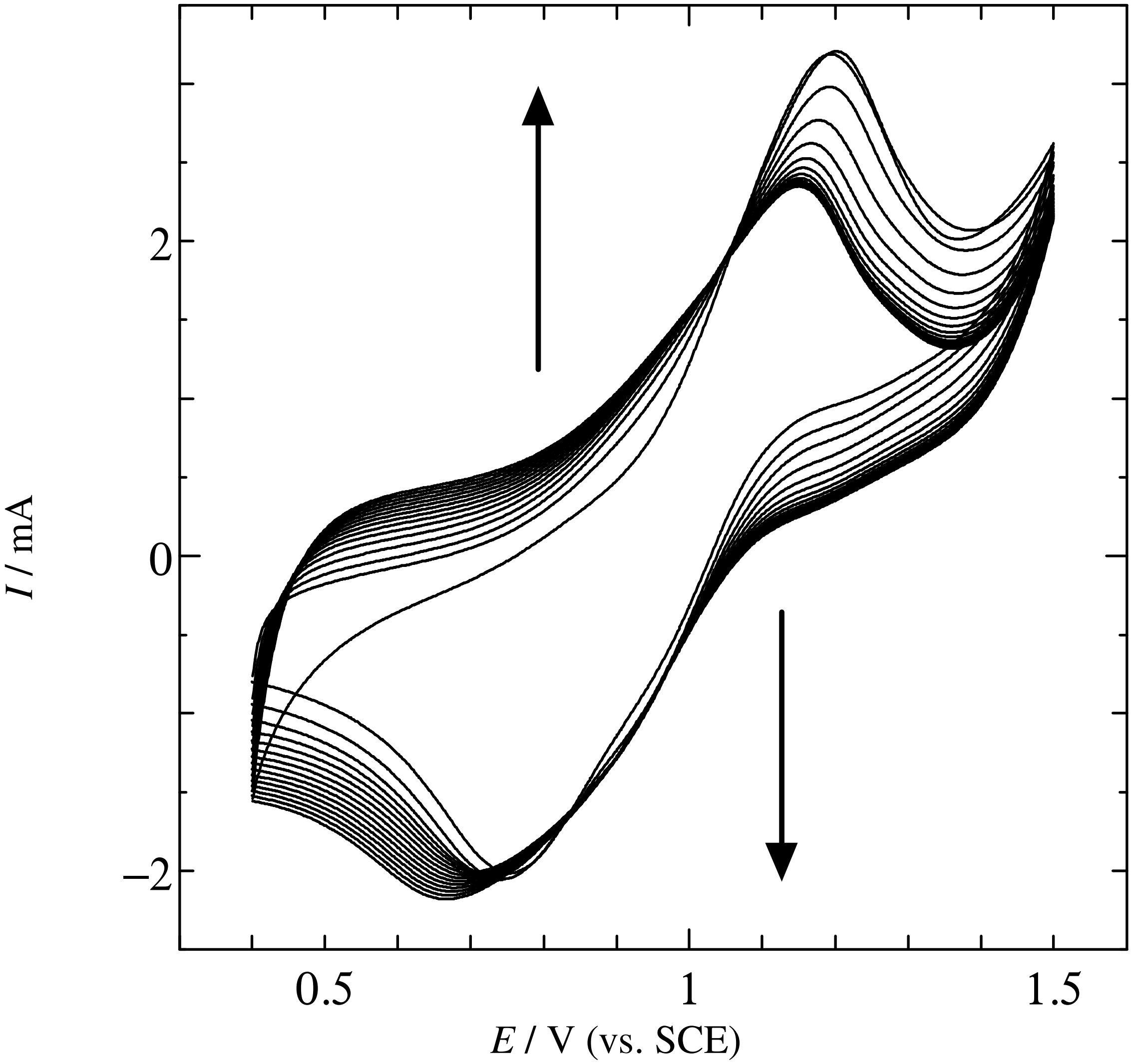

Figure 1. CVs obtained on a graphite electrode in 0.1 M Na_2SO_4 aqueous solution containing 5 mM $MnSO_4$ at 20 mV s^{-1} for 15 cycles.

3. RESULTS AND DISCUSSION

3.1 Preparation of Pd/MnO$_2$-modified graphite electrode

Typical cyclic voltammograms (CVs) obtained in a Na_2SO_4 solution with 5 mM $MnSO_4$ are presented in Fig. 1. It can be seen that both the oxidation peak current and the reduction peak current are greatly enhanced with the potential scanning cycle number. As shown in Fig. 1, the oxidation peak is more shaper than its corresponding reduction peak, i.e., the oxidation peak and its reduction peak are not symmetrical. For example, for the first cycle, the oxidation peak current is about 2.34 mA and its peak potential is located at around 1.15 V vs SCE, while its corresponding reduction peak potential is about 0.72 V with a peak current of around 1.99 mA. Theoretically, for the one-electron involved reversible electrochemical reaction, the potential separation, i.e., ΔE_p ($\Delta E_p = E_{pa} - E_{pc}$, in which E_{pa} is the anode peak potential and E_{pc} the cathode peak potential), should be 59 mV, and the ratio of anodic peak current (I_{pa}) to the cathodic peak current (I_{pc}) should be close to unit [22], therefore, it is reasonable to conclude that the electrochemical oxidation reaction of Mn^{2+} is a quasi-reversible reaction rather than a reversible one. Based on the previous report [23], As it is known, it is easy for Mn^{3+} to disproportionation in water, forming Mn^{2+} and MnO_2, i.e., $Mn^{2+} \rightarrow Mn^{3+}$, and then, $2Mn^{3+} + 2H_2O \rightarrow Mn^{2+} + MnO_2 + 4H^+$, especially in the neutral or acidic solution, thus, a typical EC process (i.e., an electrochemical reaction followed by a chemical reaction) was displayed in the electrochemical oxidation of Mn^{2+} process as shown in Fig. 1. Thus, we can attribute the broad reduction peak and the attenuated reduction peak current to the disproportion of Mn^{3+}, that is to say, Mn^{3+} was consumed by the following chemical reactions, leading to the formation of manganese dioxides on the surface of the graphite electrode [24].

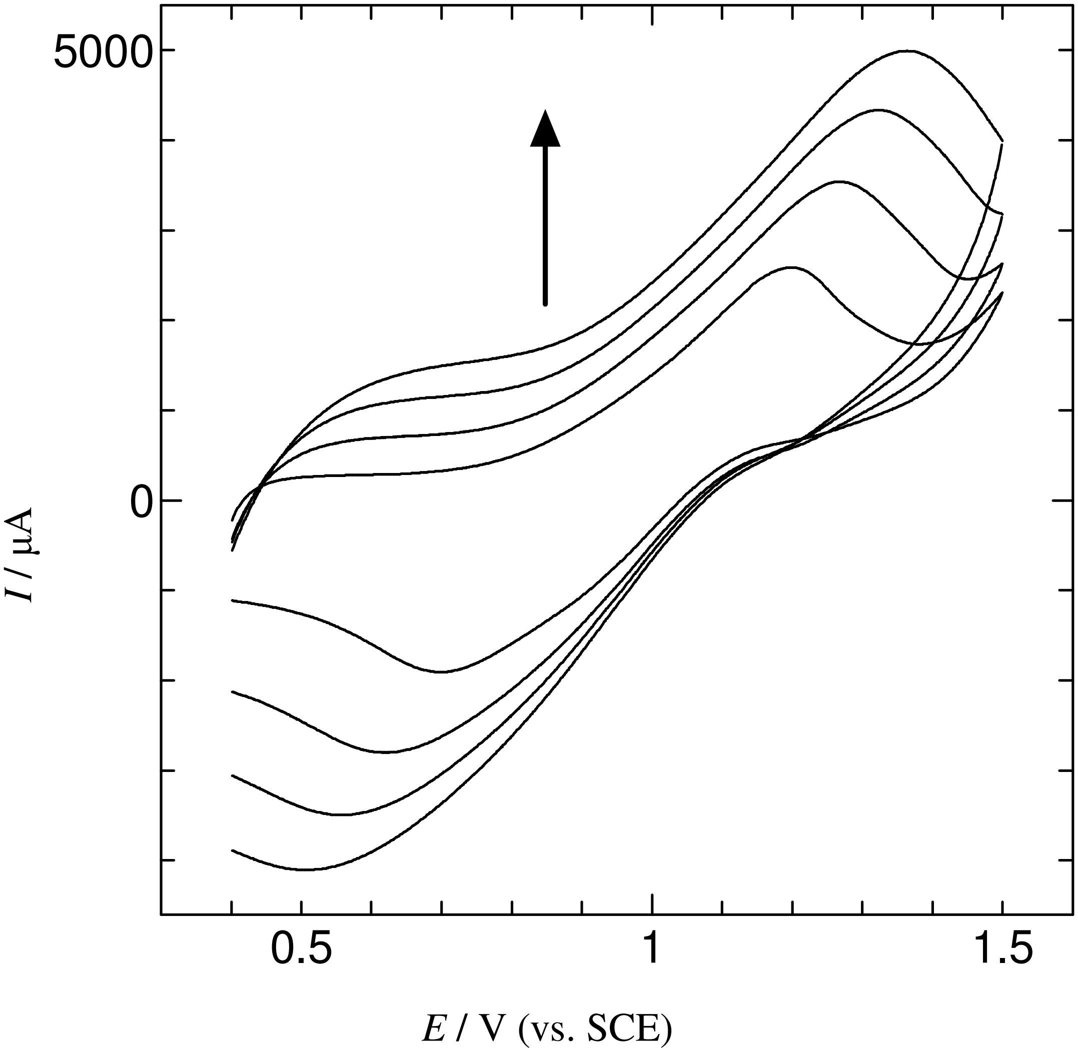

Figure 2. CVs obtained on a graphite electrode in 0.1 M Na_2SO_4 aqueous solution containing 5 mM $MnSO_4$ at various scan rates. As shown by the arrow, the scan rate are 50,100, 150, 200 mVs^{-1}, respectively.

CVs of Mn^{2+} at different scan rates are shown in Fig.2. It can be seen that with the increase of potential scan rate, the oxidation peak current, and the reduction peak current are greatly increased. And a well-defined linear relationship between the oxidation peak current and the square root of scan rate was acquired (data was not shown here), suggesting that the electrochemical oxidation reaction of Mn^{2+} was dominated by a diffusion-controlled process. Also, it is can be seen that with the increase of potential scan rate, the oxidation peak potential was positively shifted greatly, i.e., the electrochemical oxidation of Mn^{2+} became more difficult as the potential scan rate was increased, indicating that the polarization potential of the working electrode was increased probably due to the formation of MnO_2 on the surface of the graphite electrode. Thus, according to the oxidation peak potential, it can be confirmed that manganese dioxides were formed on the surface of the graphite electrode.

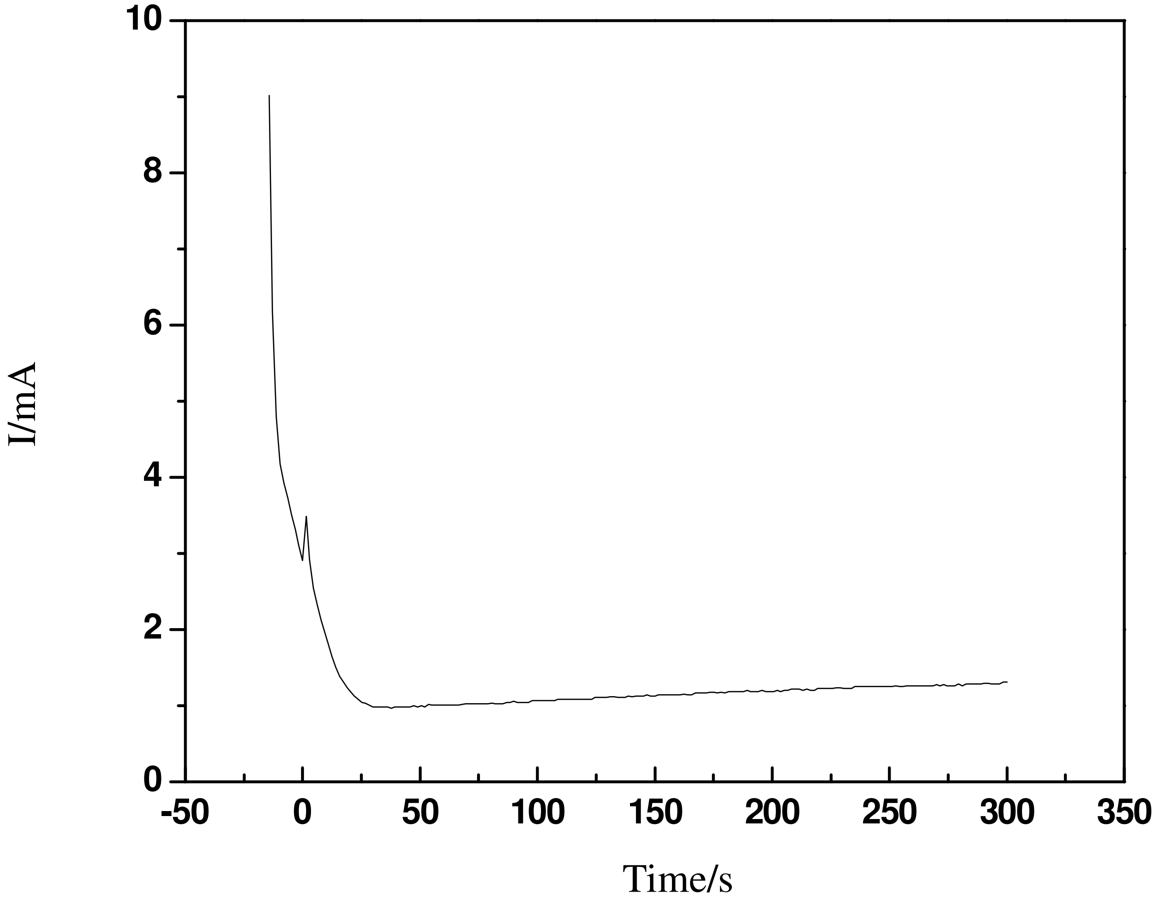

Figure 3. Curve of current against time when the electrode potential of working electrode was kept to be -0.3 V vs. SCE for 300 s.

The potentiostatic plot, i.e., the curve of current against time, is presented in Fig. 3 clearly. It should be noted that when an electrochemical reduction is expected, the electrode potential of the working electrode must be controlled to be a negative potential value compared to the open circuit potential (OCP). Here, in this preliminary work, after many attempts, -0.3 V was employed since the OCP of the MnO_2-modified graphite electrode is close to 0 V vs SCE. Additionally, it should be mentioned that the current exhibited in Fig. 3 is the current existing between the working electrode of MnO_2-modified graphite electrode and the auxiliary electrode. From Fig. 3, it can be seen that in the duration time, the current decreased dramatically especially at the beginning part of I-t curve, and then a steady current plot was exhibited. Interestingly, there is a small current peak at 2.5 s with a current value of about 3.0 mA, indicating that probably there is a nucleation formation process corresponding to the reduction of Pd^{2+}, i.e., $Pd^{2+}+2e \rightarrow Pd$ [25]. More interestingly, for the steady part of I-t curve, the current value gradually increased with the duration time rather than attenuation. For example, at 100 s the current is 1.02 mA, while at 200 s the current is 1.14 mA, implying that some substances with higher conductivity were formed on the surface of the MnO_2-modified graphite electrode. Therefore, Fig. 3 strongly verified that some substances were prepared on the resultant MnO_2-modified graphite electrode, though there are many modes to explain the nucleation formation process [26].

3.2 Characterization of Pd/MnO_2 composite materials

Fig. 4 is the images for the obtained samples. Image A is the image of the pure MnO_2 in which irregular particles were observed, similar to the reported images of MnO_2 [27]; image B is the image of the Pd-coated MnO_2 in which some black dots are exhibited on the surface of MnO_2. The inset of image B is the magnified image B, in which magnified black dots-like particles are clearly observed. Fig. 4 demonstrates that some substances were formed on the surface of the resultant MnO_2 after the potentiostatic electrodeposition process as described in Fig. 3.

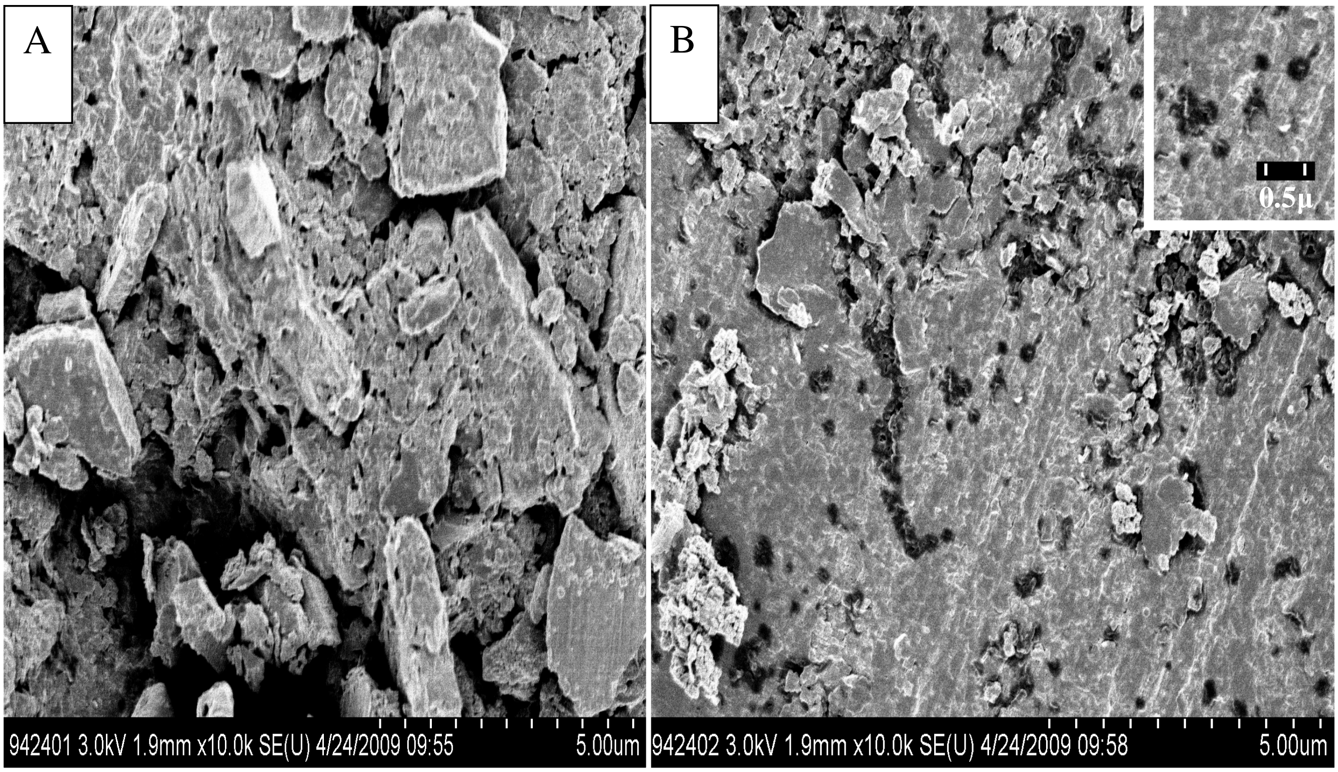

Figure 4. SEM images of the obtained samples. Image A: MnO_2; image B: Pd-coated MnO_2. The inset is the magnified image B.

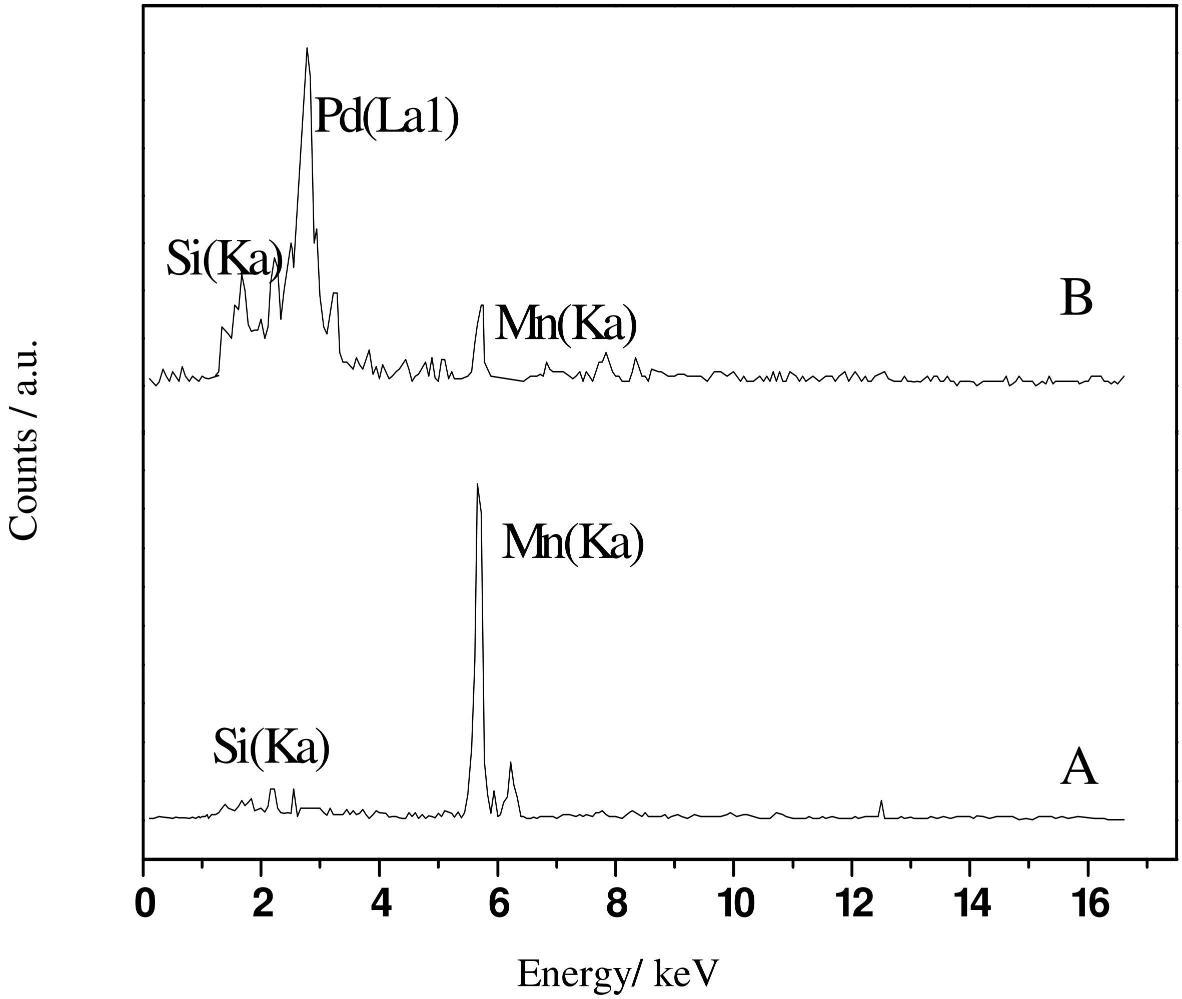

Figure 5. EDX spectra for the obtained samples. Line A: MnO_2; line B: Pd-coated MnO_2.

Fig. 5 is the EDX spectra for the obtained samples. Line A is the spectrum corresponding to the pure MnO_2, consistent with the former report very well [28]. After electrodeposition, the peak corresponding to Pd element is exhibited. Moreover, except for Pd element, no other elements were found, suggesting that only Pd particles are formed on the surface of MnO_2.

Fig. 4 and Fig. 5 strongly indicate that Pd particles were formed on the surface of MnO_2, though our prepared Pd particles are larger than those reported previously [6]. Our work indicates that potentiostatic method is a feasible technique to fabricate Pd particles, as is reported for the first time so far. Evidently, there are many factors affect the resultant samples, such as the applied potential, the duration time, the electrolyte solution employed, and so on. Further investigations are in progress.

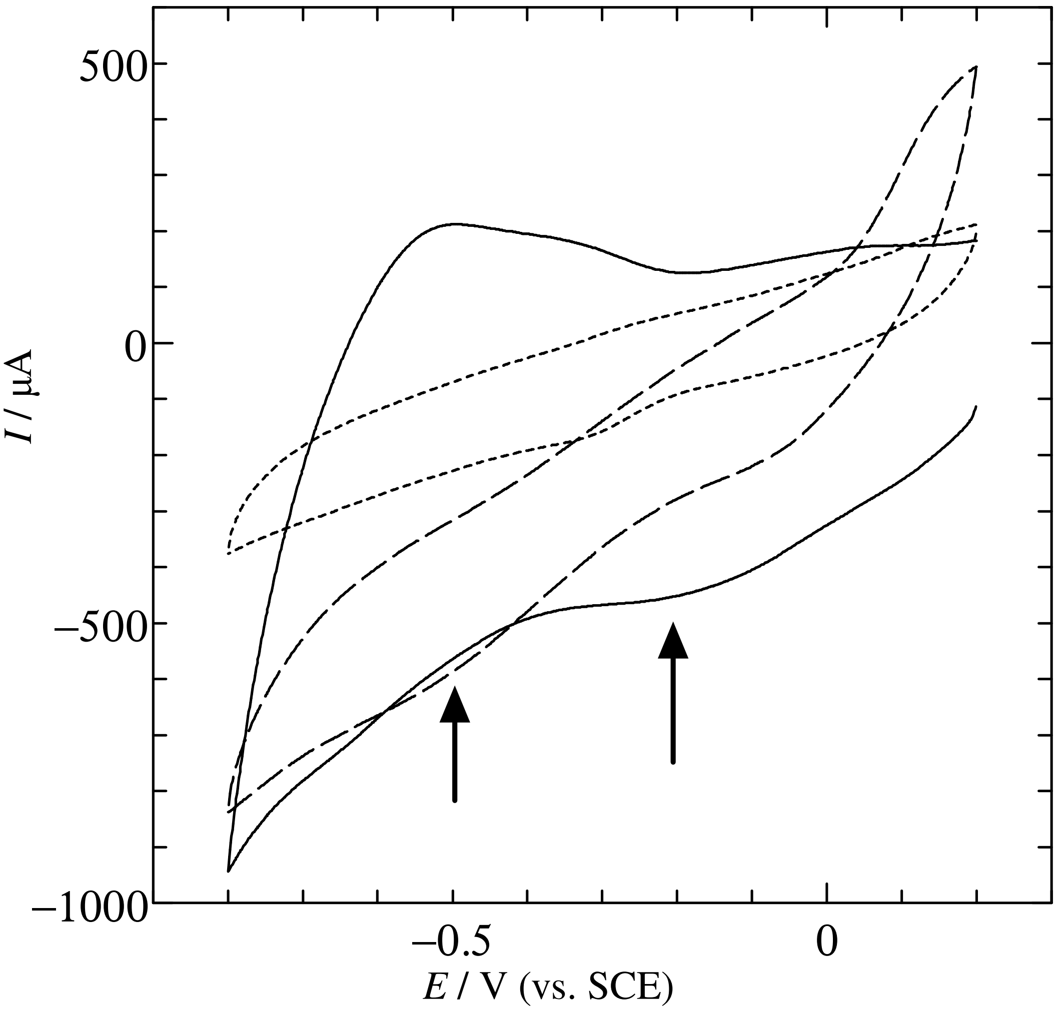

Figure 6. CVs of ORR on a graphite electrode in an oxygen-saturated 0.1M Na_2SO_4 solution. Dotted line: obtained on a graphite electrode; dashed line: on a MnO_2-coated graphite electrode; solid line: obtained on a Pd/MnO_2-coated graphite electrode. Scan rate: 20 mV s^{-1}.

3.3 Catalysis of Pd/MnO_2 towards oxygen reduction reaction (ORR)

As stated above, ORR is the only one reaction happened on the cathode of fuel cells, though many kinds of fuel cells were developed, e.g., PEMFC, DMFC, and DEFC. Therefore, exploring the catalyst for ORR is a main task for electrochemistry researchers. Pd-based catalyst for ORR has been well reported [29, 30]. Fig. 6 is the CVs obtained in an oxygen-saturated 0.1 M Na_2SO_4 aqueous solution, in which the dotted line was recorded on a graphite electrode, while the dashed line was plotted based on the MnO_2-coated graphite electrode, and the solid line was procured on the Pd/MnO_2-modified graphite electrode. Obviously, a reduction peak was exhibited on the Pd/MnO_2-modified graphite electrode though it was small. Moreover, it showed that the reduction peak potential of ORR on the MnO_2-coated electrode greatly positively shifted. For instance, on the MnO_2-coated electrode, the reduction peak potential is about -0.5 V, while on the Pd/MnO_2-coated electrode, the reduction peak potential shifted to be around -0.2 V (as shown by the arrows in Fig. 6). To confirm the origin of the reduction peak in Fig. 6, CVs in various solutions were shown in Fig. 7. In Fig. 7, the dotted line was obtained in the nitrogen-saturated 0.1 M Na_2SO_4 aqueous solution, in which no reduction peak was observed. The solid line was obtained in an oxygen-saturated 0.1 M Na_2SO_4 aqueous solution, where an evident reduction peak was exhibited, hence, it is rational to confirm that the reduction reaction occurring at about -0.2 V should be the reduction of oxygen molecules rather than the reduction of MnO_2 or other substances. Due to the disporporation of superoxide anion, i.e., O_2^-, the reduction product of oxygen molecule, no oxidation peak of superoxide anion O_2^- was exhibited, rather different from the redox behavior of oxygen molecules in room temperature ionic liquids (RTILs) [21].

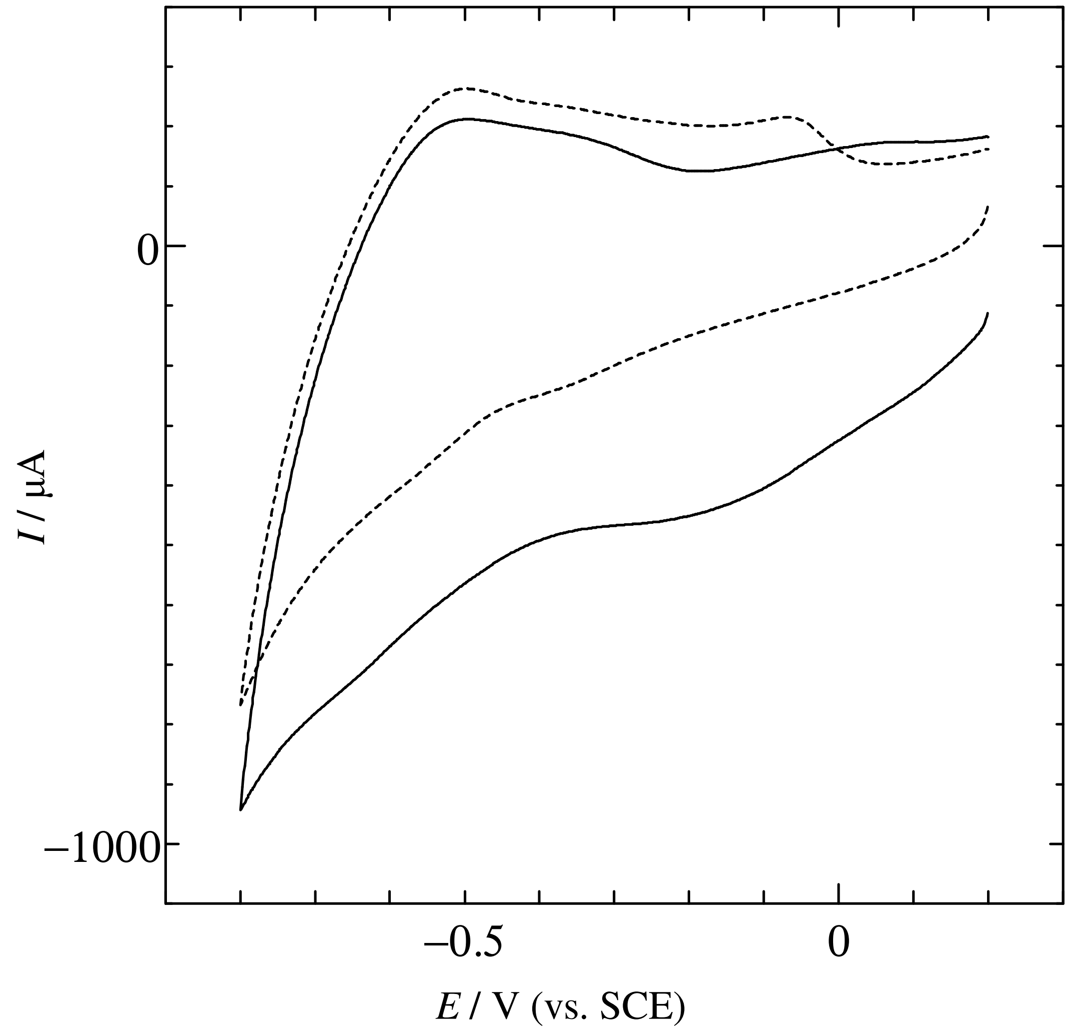

Figure 7. CVs of ORR on a Pd/MnO_2-coated graphite electrode in 0.1M Na_2SO_4 solution. Dotted line: obtained in a nitrogen-saturated solution; solid line: obtained in an oxygen-saturated solution. Scan rate: 20 mV s^{-1}.

Fig. 8 is CVs of ORR obtained on a Pd/MnO_2-coated graphite electrode in an oxygen-saturated 0.1 M Na_2SO_4 aqueous solution at different scan rates. Evidently, the oxygen reduction peak current gradually increased with increasing potential scan rates, very similar to the reported CVs of ORR on carbon nanofibers (CNF) [31]. A linear relationship between the reduction peak current and the square root of scan rate was also obtained (data was not shown here), suggesting that the reduction reaction of oxygen molecules is a diffusion-controlled process, also supporting that the reduction reaction at around -0.2 V was the reduction of oxygen molecules. Therefore, above figures strongly demonstrated that ORR could proceed on this developed Pd/MnO_2-coated graphite electrode, indicating that it is possible to apply the developed Pd/MnO_2 material in the fuel cells.

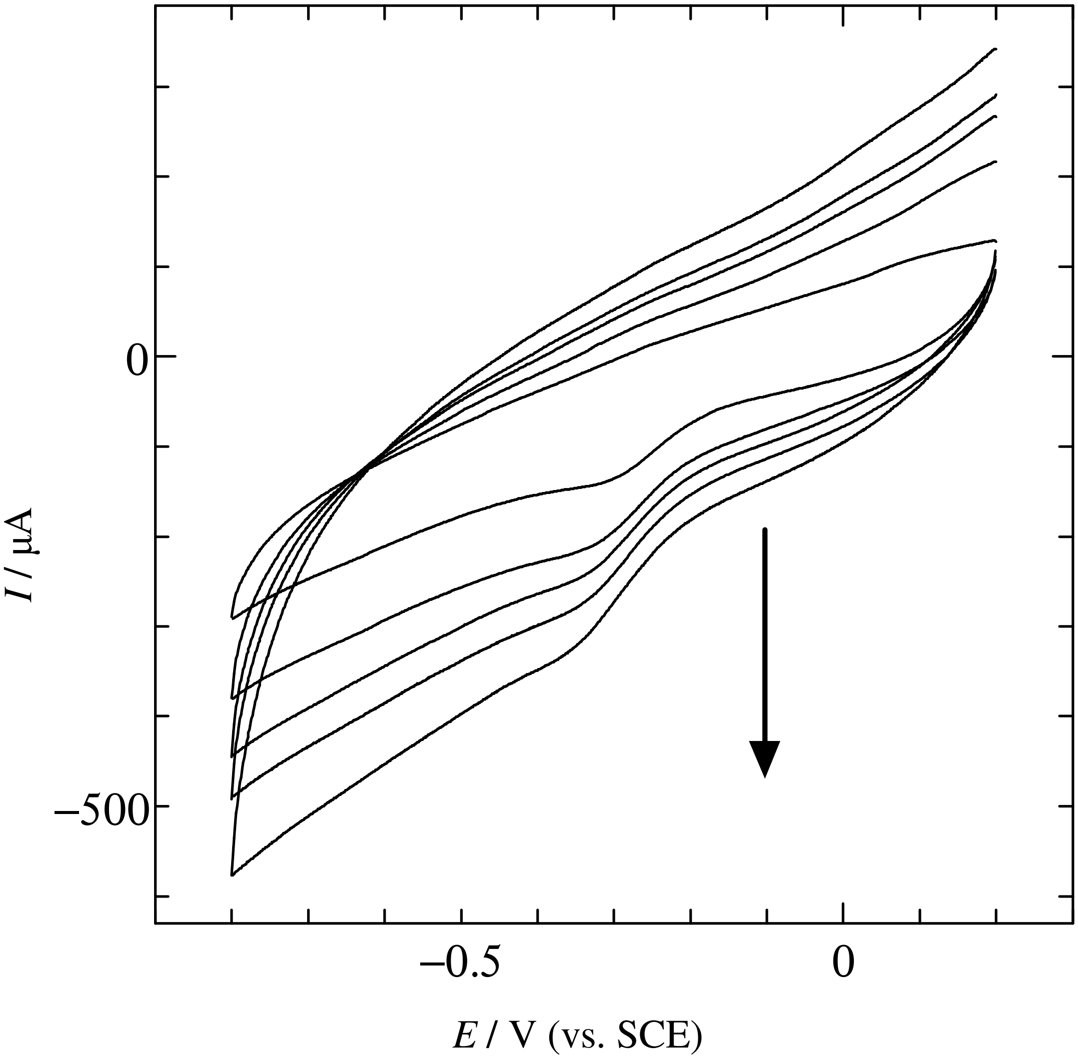

Figure 8. CVs of ORR on a Pd/MnO_2-coated graphite electrode in an oxygen-saturated 0.1 M Na_2SO_4 solution at different scan rates. As shown by the arrow, scan rates are: 20, 50, 80, 100, 150 mV s^{-1}.

Electrochemical impedance spectroscopy (EIS) is a widely used method to describe the metal oxide coated on an electrode surface [32]. Fig. 9 presents typical Nyquist plots obtained at 0 V versus SCE over the frequency range from 1Hz to10^5 Hz. It can be seen that the plot corresponding to pure

MnO_2 was composed of a semicircle at high and intermediate frequencies and a perpendicular line at the low frequencies regions, consistent with the previously reported results very well [33].

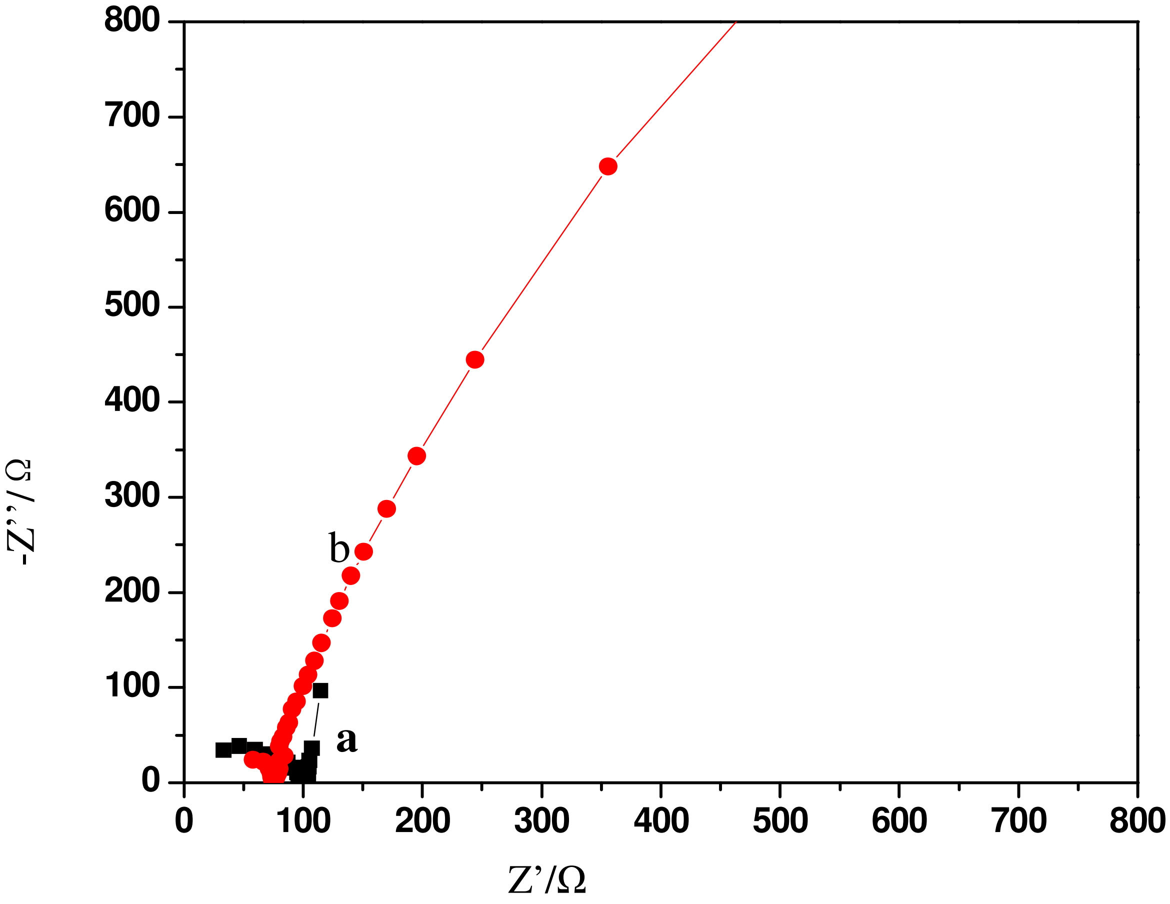

Figure 9. Nyquist plots obtained in an oxygen-saturated 0.1 M Na_2SO_4, line **a**: obtained for the MnO_2-modified graphite electrode; line **b**: for a Pd/MnO_2-modified graphite electrode.

Generally, there should be a line perpendicular to the real part of resistance (Z') for the pure capacitance element, and the semicircle, exhibited in Nyquist plots as shown in the high frequency regions of Fig.9, is usually interpreted as a capacitance element in parallel with a resistance element[34]. it was widely accepted that the semicircle with a larger diameter corresponds to a higher charge transfer resistance (R_{ct}) [35], thus one can see that for the Pd/MnO_2 composite material, the semicircle displayed in the high frequencies region became smaller when compared to the pure MnO_2, indicating that the charge transfer resistance was lowered by the modification of Pd particles. That is to say, the charge transfer rate was accelerated by the Pd particles on the surface of MnO_2. Moreover, for the Pd/MnO_2 composite material, the line appearing at the lower frequencies region is a 45° line rather than a 90° line, implying that the diffusion process on the Pd/MnO_2 composite material was greatly strengthened when compared to the case on the pure MnO_2 since the 45° line corresponds to a Warburg diffusion process [35]. We must admit that due to the complexity of manganese oxides, Nyquist plot can only reflect the whole change of working electrode, unable to provide the interpretation quantitatively.

As for the catalysis of Pd for ORR, there are several propositions published so far. For example, Yang [29] has addressed that there are three different reactions occurring, i.e., 4e$^-$ reduction, 2e$^-$ reduction and the reduction of intermediate HO_2^- when oxygen molecules were reduced on a Pd surface. Lin [6] pointed that oxygen molecule tends to form a complex $Pd^{\delta+}(O_2)^{\delta-}$ on the surface of palladium nanoparticles and negatively charged oxygen atoms could interact with protons to form H_2O_2. He also proposed that the complex of $Pd(H_2O_2)$ may be the intermediates in the process of oxygen reduction. Meanwhile, Hu [36] reported a highly sensitive hydrogen peroxide amperometric sensor based on MnO_2 nanoparticles, in which MnO_2 is reduced to lower states by H_2O_2, i.e., $MnO_2 + H_2O_2 \rightarrow MnO(orMn_2O_3) + H_2O$.

Thus, based on above mechanisms [6, 36], we think, on the Pd/MnO_2 composite materials, probably, ORR proceeds via the following modified paths.

$$O_2 + Pd + \delta e^- \rightarrow Pd(O_2)^{\delta-} \quad (1) \text{ (Electrochemical reaction)}$$
$$O_2^{\delta-} + H^+ \rightarrow H_2O_2 \quad (2)$$
$$Pd + H_2O_2 \rightarrow Pd(H_2O_2) \quad (3)$$
$$Pd(H_2O_2) + MnO_2 \rightarrow Pd + MnO(orMn_2O_3) + H_2O \quad (4) \text{ (Chemical reaction)}$$

That is to say, on this novel material of Pd/MnO_2, an EC process happened, in which Pd particles were used as substrate on which electrochemical reactions occurred, and MnO_2 was employed as an oxidative reagent to oxidize the intermediate produced in the process of oxygen reduction. Since the process of ORR is very complicated, there are many factors affecting its mechanism [37, 38], such as the electrolyte, the substrate, etc. More works are required to show a satisfied interpretation on the catalysis of Pd/MnO_2 towards ORR. Further works are also in progress in our lab.

4. CONCLUSIONS

In this work, palladium particles-decorated manganese dioxide-modified graphite electrode was generated by a combination of CV and potentiostatic methods, which was verified by the obtained SEM images and EDX spectra. The obtained cyclic voltammograms (CVs) indicated that the developed composite material of Pd/MnO_2 has higher electrocatalytic activity towards ORR when compared to the pure MnO_2 materials. The possible mechanism of Pd/MnO_2 towards ORR was also proposed based on our date and previously published works.

ACKNOWLEDGEMENTS
This work was financially supported by the Doctor Fund of Hebei Normal University (L2003B10), Key Project of Hebei Normal University (L2008Z08), Key Project of Hebei Province Education Bureau (ZH2007106) and Special Assist Project of Hebei Province Personnel Bureau (106115)

References

1. N. Tian, Z. Y. Zhou, S. G. Sun, Y. Ding, Z. L. Wang, *Science* 316(2007)732.
2. V. Komanicky, H, Iddir, K.-C. Chang, K.-C. Chang, A. Menzel, G. Karapetrov, D. Hennessy, P. Zapol, H. You, *J. Am. Chem. Soc.* 131(2009) 5732.
3. K.-Q. Ding, M. Cao, *Russ. J. Electrochem.* 44(2008) 977.
4. C. Coutanceau, L. Demarconnay, C. Lamy, J.-M. Léger, *J. Power Sources* 156(2006) 14.
5. W. J. Zhou, S. Q. Song, W. Z. Li, Z.H. Zhou, G.Q. Sun, Q. Xin, S. Douvartzides, P. Tsiakaras, *J. Power Sources* 140 (2005) 50.
6. Y. Lin, X. Cui, X. Ye, *Electrochem. Commun.* 7(2005) 267.
7. Z. Liu, X. Zhang, L. Hong, *Electrochem. Commun.* 11(2009) 925.
8. Z. X. Liang, T.S. Zhao, J.B. Xu, L.D. Zhu, *Electrochim Acta* 54(2009) 2203.
9. L. Zhang, K. Lee, J. Zhang, *Electrochim. Acta* 52(2007) 3088.
10. F. Jia, K.-W. Wong, R. Du, *Electrochem. Commun.* 11(2009) 519.
11. X.-G. Zhang, Y. Murakami, K. Yahikozawa, Y. Takasu, *Electrochim. Acta* 42(1997) 223.
12. A. Mourato, J. P. Correia, H. Siegenthaler, L. M. Abrantes, *Electrochim. Acta* 53(2007) 664.
13. S. Pandelov, U. Stimming, *Electrochim. Acta* 52(2007) 5548.
14. P. Zóltowski, D. M. Drazić, L. Vorkapić, *J. Appl. Electrochem.* 3(1973) 271.
15. L. Mao, D. Zhang, T. Sotomura, K. Nakatsu, N. Koshiba, T. Ohsaka, *Electrochim. Acta* 48(2003) 1015.
16. K.-Q. Ding, *J. Chin. Chem. Soc.* 55(2008) 543.
17. K.-Q. Ding, *Int. J. Electrochem. Sci.* 5(2010) 72.
18. L. Zhang, Z. Fang, Y. Ni, G. Zhao, *Int. J. Electrochem. Sci.* 4(2009) 407.
19. K.-Q. Ding, F.-M. Cheng, *Synth. Met.* 159(2009):2122.
20. M. S. El-Deab, T. Ohsaka, *Electrochim. Acta* 52(2007) 2166.
21. K.-Q. Ding, T. Okajima, T. Ohsaka, *Electrochemistry* 75(2007) 35.
22. C. Hu, S. Yuan, S. Hu, *Electrochim. Acta* 51(2006)3013.
23. J. Ph. Petitpierre, Ch. Comninellis, E. Plattner, *Electrochim. Acta* 35(1990) 281.
24. N. Nagarajan, M. Cheong, I. Zhitomirsky, *Mater. Chem. Phys.* 103(2007) 47.
25. J. N. Broughton, M. J. Brett, *Electrochim. Acta* 50(2005) 4814.
26. C. Bjelkevig, J. Kelber, *Electrochim. Acta* 54(2009)3892.
27. C.-C. Hu, T.-W. Tsou, *Electrochim. Acta* 47(2002) 3523.
28. K. R. Prasad, N. Miura, *J. Power Sources* 135 (2004) 354.
29. Y.-F. Yang, Y.-H. Zhou, C.-S. Cha, *Electrochim. Acta* 40(1995)2579.
30. X. Li, Q. Huang, Z. Zou, B. Xia, H. Yang, *Electrochim. Acta* 53 (2008) 6662.
31. J.-S. Zheng, X.-S. Zhang, P. Li, X.-G. Zhou, D. Chen, Y. Liu, W.-K. Yuan, *Electrochim. Acta* 53(2008) 3587.
32. J. Gamby, P. L. Tabema, P. Simon, J. F. Fauvarque, M. Chesneau, *J. Power Sources* 101(2001) 109.
33. S.-E. Chun, S.-I. Pyun, G.-J. Lee, *Electrochim. Acta* 51(2006) 6479.
34. K.-Q. Ding, Z. Jia, Q. Wang, X. He, N. Tian, R. Tong, X. Wang, *J. Electroanal. Chem.* 513(2001) 67.
35. K.-Q. Ding, Q. Wang, Z. Jia, R. Tong, X. Wang, H. Shao, *J. Chin. Chem. Soc.* 50(2003) 387.
36. S. Yao, J. Xu, Y. Wang, X. Chen, Y. Xu, S. Hu, *Anal. Chim. Acta* 557(2006) 78.
37. Y. Lu, H. Xu, J. Wang, X. Kong, *Electrochim. Acta* 54(2009) 3972.
38. A. Sarapuu, A. Kasikov, T. Laaksonen, K. Kontturi, K. Tammeveski, *Electrochim. Acta* 53(2008) 5873.